

BARRIER CROSSING THEORY FOR ULTRA-FINE DETAIL IN THE FAR INFRA-RED ABSORPTION
OF DIPOLAR LIQUIDS

M.W. EVANS^{*}, C.J. REID[†], J. ABAS^{**} and G.J. EVANS⁺⁺

^{*} Department of Physics, U.C.N.W., Bangor, Gwynedd, Wales

[†] Department of Chemistry, Llandyfri College, Llanymddyfri, Dyfed, Wales

^{**} Department of Applied Mathematics, U.C.N.W., Bangor, Gwynedd, Wales

⁺⁺ Department of Chemistry, U.C.W., Aberystwyth, Dyfed, Wales

ABSTRACT

The recent suggestion of ultra-fine detail in the far infrared power absorption of liquid acetonitrile (G.J.E.) is given support with a theory of rotational Brownian motion in cosine potential wells in the low friction limit. The theory and algorithm developed by Reid is used in this limit to produce a series of sharp absorptions in the far infrared as a function of well depth and multiplicity. With a multiplicity of 2 as many as eleven peaks are already observable which vary considerably in position and relative intensity with barrier height and temperature. The role of friction increasing is to broaden the individual peaks of the fine structure into a broad, continuous absorption profile - a "conventional" far infra-red power absorption profile [1,2]. The same model produces a broad dielectric loss curve at lower frequencies in accord with experimental observation (1.12 decades of frequency half-width). A preliminary investigation of the effect of an external electric field is made with the use, effectively, of a complex friction coefficient. Again the results appear to support the experimental observations of G.J.E. The theory provides strong evidence supporting an hypothesis [12] that the far infrared spectra of dipolar liquids are complex, composite profiles.

INTRODUCTION

The far infra-red power absorption profile of a dipolar liquid is conventionally [1] thought of as a very broad band, of half-width typically 50 to 80 cm^{-1} , extending to about 200 or 300 cm^{-1} . If we convert power absorption ($\alpha(\omega)$ in neper cm^{-1}) to dielectric loss ($\epsilon''(\omega)$) then the

frequency dependence of the latter is conventionally a bell-shaped curve peaking at much lower frequencies in the MHz or GHz region. This grossly simplified description is the product of historical accident. Use of two different methods for recording the absorption as a function of frequency (i.e. of $\alpha(\omega)$ and $\epsilon''(\omega)$) adds to the confusion. In fact these are linked through the Maxwell equations by:

$$\alpha(\omega) = \omega \epsilon''(\omega) / n(\omega) \quad (1)$$

where $n(\omega)$ is the frequency dependent refractive index. Therefore an understanding in terms of molecular dynamics of these frequency dependent processes must involve both $\alpha(\omega)$ and $\epsilon''(\omega)$ self-consistently [1]. The first attempt, by Debye, was equivalent, essentially speaking to the use of a rotational Langevin equation. In 2 - D this is [2]:

$$I \ddot{\theta}(t) + I\beta \dot{\theta}(t) = \dot{W}(t) \quad (2)$$

where I is the effective molecular moment of inertia, β the friction coefficient, and $\dot{W}(t)$ the random torque on a molecule due to its surroundings - in modern terms a Wiener process [3]. The rotational motion of the molecule is described by one coordinate, θ , for the sake of simplicity. The fuller 3 - D versions of eqn. (2) have been considered in great detail [4], but do not tell us much more about the frequency dependence of α or ϵ'' . The solution of eqn. (2) for the angular velocity and orientational autocorrelation functions are well-known to be, respectively [5]:

$$\langle \dot{\theta}(t) \dot{\theta}(0) \rangle = e^{-\beta t} \quad (3)$$

$$\langle \cos\theta(t) \cos\theta(0) \rangle = \exp - \frac{kT}{I\beta^2} (\beta t - 1 + e^{-\beta t}) \quad (4)$$

Debye assumed effectively that $\beta \gg \ddot{\theta}(t)/\dot{\theta}(t)$ in eqn. (2), and therefore worked in a "high friction" limit, where eqn. (4) reduces to:

$$\langle \cos\theta(t) \cos\theta(0) \rangle \div \exp - \left(\frac{kT}{I\beta}\right)t \quad (5)$$

i.e. the orientational a.c.f. is a simple exponential. The quantity

$$\tau_D = \frac{I\beta}{kT} \quad (6)$$

is equivalent to the "Debye relaxation time" in two dimensions. The full, 3 - D, spherical top problem provides eventually the same type of exponential, except for a numerical factor - essentially an adjustment from the effective 2 - D moment of inertia to the real 3 - D equivalent - that of the spherical top. Perrin extended Debye's approximate results to the diffusing asymmetric top, producing in the process, three relaxation times [4] of the type (5). "Inertial effects" were considered in the mid seventies with little further physical insight to what was already well known [4].

All these theories fail to describe what is readily observable, in terms of $\epsilon''(\omega)$ and $\alpha(\omega)$, in dipolar liquids. Eqn. (5) leads to the spectral disaster of the Debye plateau [1] in power absorption, $\alpha(\omega)$, and the more accurate eqn. (4) (or its 3 - D counterparts) merely ensure a return to transparency from the plateau level at high frequencies. These "one particle" theories fail to account for the existence of intermolecular potential wells, i.e. for the influence of liquid structure in molecular dynamics. This is the root-cause of the gap, which persists to the present day between the disciplines of fluid or hydrodynamics and molecular dynamics.

The attempts to close this gap originated probably with the Kirkwood school, using methods based on hydrodynamics, and with the work by Kramers [6] on Brownian motion in the presence of barriers. This work developed in the sixties in terms of linear itinerant-oscillator models [1,2]. This has recently been given a rigorous basis, and related to the stochastic Liouville equation, by Grigolini and co-workers [7]. The simplest way to introduce a potential well is to rewrite eqn. (2) as:

$$I\ddot{\theta}(t) + I\beta\dot{\theta}(t) + V'(\theta) = \dot{W}(t) \quad (7)$$

where the torque $V'(\theta)$ is the derivative of the potential energy between a molecule and its surroundings with respect to θ . The molecule is now a torsional oscillator, and fluctuations in its environment allow it to surmount occasionally, the energy barrier separating one intermolecular well from the next. This implies that the molecular liquid must be structured. The structure may be represented most simply by cosine wells of the form [8]:

$$V = -V_0 \cos(M\theta(t)) \quad (8)$$

where V_0 is the barrier height and M the well multiplicity.

If $M = 2$, for example, then there are two different sites of equal depth V_0 . A fuller generalisation could be obtained with a thermodynamic average over well-depths V_0 .

The system of equations (7) and (8) was recently solved numerically by Reid [8], by transformation into the equivalent Kramers equation [1,2,7]:

$$\frac{\partial \rho}{\partial t} + \theta \frac{\partial \rho}{\partial \theta} - \frac{V'}{I} \frac{\partial \rho}{\partial \dot{\theta}} = \beta \frac{\partial}{\partial \dot{\theta}} \left(\dot{\theta} \rho + \frac{kT}{I} \frac{\partial \rho}{\partial \dot{\theta}} \right) \quad (9)$$

for the conditional phase space probability density function $\rho(\dot{\theta}, \theta, t | \dot{\theta}(0), \theta(0), 0)$. Earlier attempts by Praestgaard et al. [9] and Risken et al. [10] used approximations which apparently removed much of the information available from eqn. (9). A slightly more sophisticated version of eqn. (9) is available in the literature [11], and was solved by a numerical method devised by Ferrario [11], analogous to that devised independently by Reid [8].

The recent suggestion by G.J. Evans [12] of a richly detailed sub-structure in the far infra-red spectrum of liquid acetonitrile has prompted us to re-examine the results by Reid in order to provide a theoretical basis for further experimental investigation of this kind, possibly with supplementary spectroscopic techniques. This paper is a description of some of these results, obtained from the "Schrodinger" type equation (9) by reducing it, following Reid [8], to a matrix equation ("Heisenberg" type) solved subject to equilibrium initial conditions on the probability density function ρ . The experimental results by Evans [12] refer to acetonitrile, a liquid whose viscosity at room temperature is among the lowest recorded, and whose equilibrium structure is known to be pronounced [13]. This suggests that eqn. (9) should be solved in the low friction limit, because of the linear relation between friction coefficient and viscosity [1]. The observed structural properties of acetonitrile [14] suggest that the barrier height V_0 should reflect the number of well-sites available to the molecule - the diffusing torsional oscillator. The effective moment of inertia I should represent in some way a well-known characteristic of the acetonitrile molecule - the fact that the principal moment of inertia about the C_{3v} axis is about 10 times smaller than its two mutually perpendicular counterparts [14]. With these provisos the analysis based on the Kramers eqn. (9) should be able to produce, qualitatively, the far infra-red fine structure. A fully quantitative assessment would involve a more realistic estimate of the intermolecular potential [14] and distribution of well-depths in eqn. (9).

Finally the effect of an external electric field is reportedly (G.J.E., figure 1), to sharpen the peaks and promote the appearance of further fine detail. This may be described analytically with the Langevin equation [15]:

$$I\ddot{\theta}(t) + I(\beta - i\omega_1)\dot{\theta}(t) + V'(\theta) = \dot{W}(t) \quad (10)$$

where $\omega_1 = (\frac{\mu E}{I})^{1/2}$, μ being the molecular dipole moment and E the external electric field strength. The solution of eqn. (10) follows that of eqn. (7) with β replaced everywhere by $(\beta - i\omega_1)$ - in effect a complex friction coefficient. Results are presented systematically, using computer graphics, as a function of ω_1 .

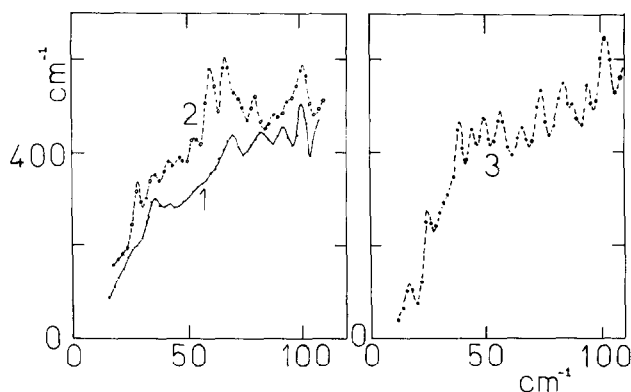
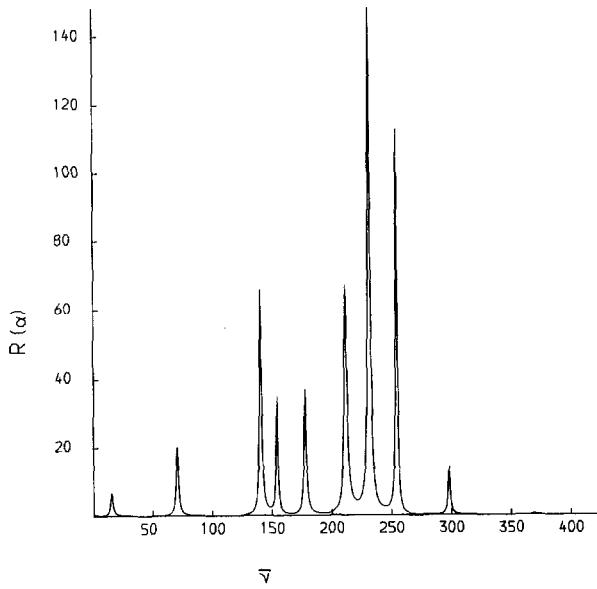


Fig. 1 Experimental results. 1) Far infra-red power absorption coefficient of liquid acetonitrile at 296 K; 2) Effect of an electric field, $E = 1 \text{ kv cm}^{-1}$; 3) 3 kv cm^{-1} .
Ordinate $\alpha(\bar{\nu} = \omega/(2\pi c))$ /neper cm^{-1} ; Abcissa: $\bar{\nu}/\text{cm}^{-1}$

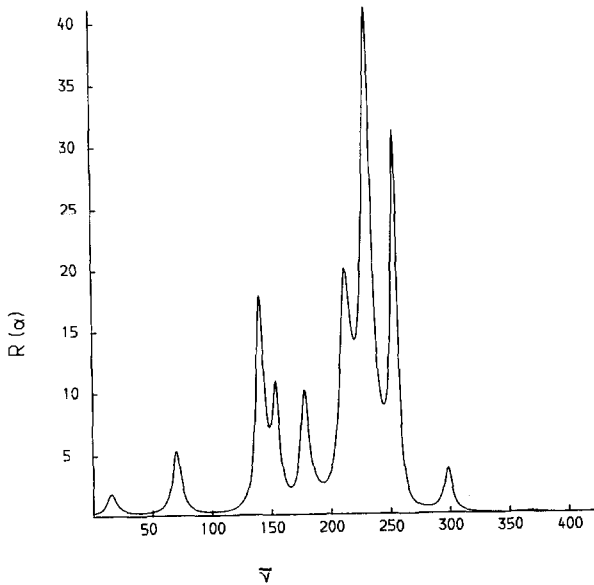
Finally in fig. (4) the effects of varying $\gamma = V_0/(IkT)^{1/2}$ is illustrated by reference to the power absorption coefficient $\alpha(\omega)$. In the "classical" (broad band) limit, with β in the region of 10 THz or more, the effect of varying γ has been discussed by Reid [8]. This is to shift the peak in the power absorption coefficient to higher frequencies, and sharpen the overall profile. At the same time the peak in the dielectric loss is shifted to lower frequencies (see table 2 of Reid's paper), so that the Debye time

$$\alpha=8, \beta=0.05, \gamma=10, N=2$$



2 a

$$\alpha=8, \beta=0.1, \gamma=10, N=2$$



2 b

Fig. 2 (i) Power Absorption vs $\bar{\nu}/\text{cm}^{-1}$; (ii) Dielectric loss vs $\log_{10}(\omega)$.
 The effect of varying β , computer graphics (Benson plotter, DEC 10/20,
 Bangor, taking results from the UMRCC CDC 7600).

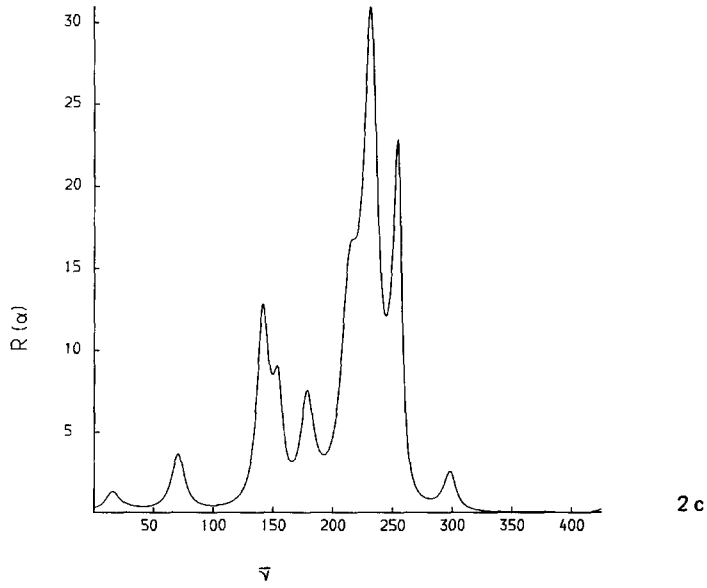
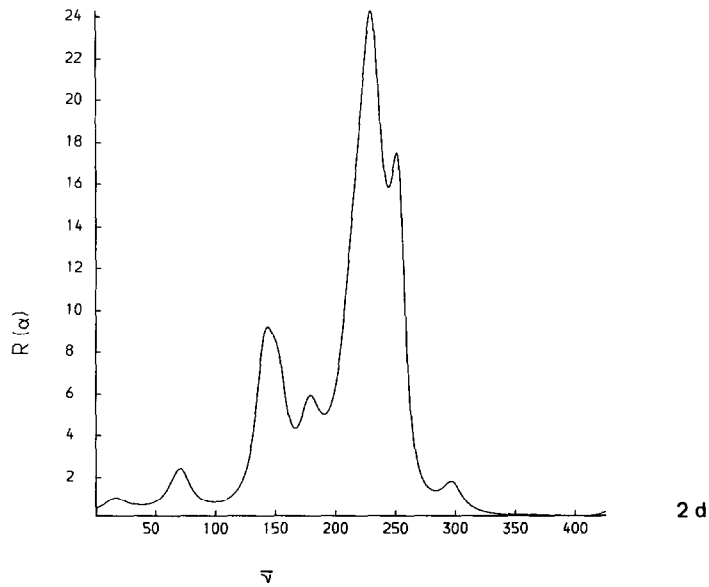
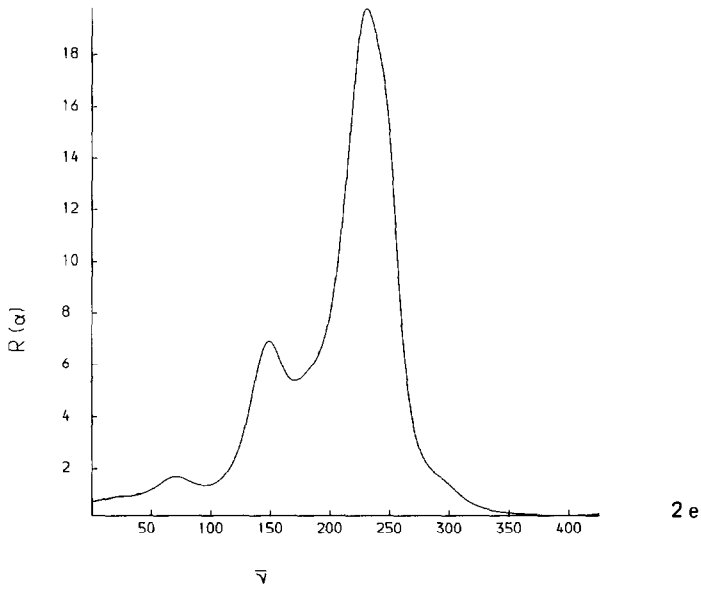
$\alpha=8, \beta=0.3, \gamma=10, N=2$  $\alpha=8, \beta=0.5, \gamma=10, N=2$ 

Fig. 2.

8

$\alpha=8, \beta=1.0, \gamma=10, N=2$



$\alpha=8, \beta=5.0, \gamma=10, N=2$

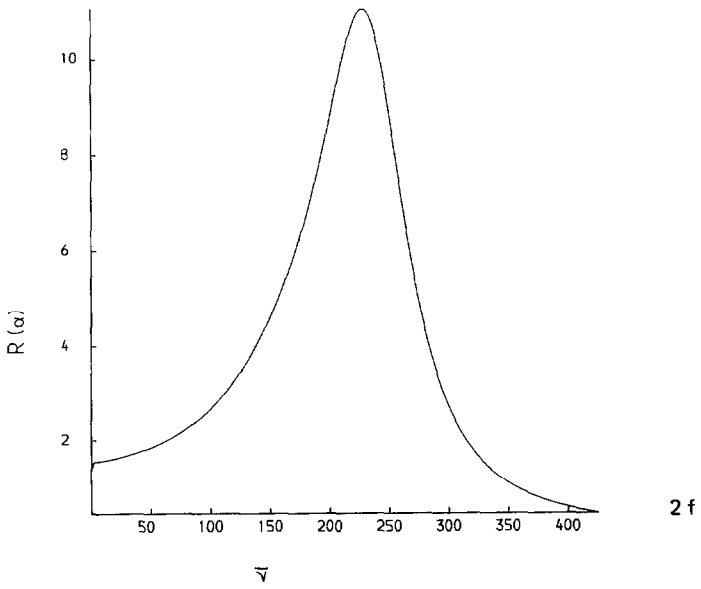
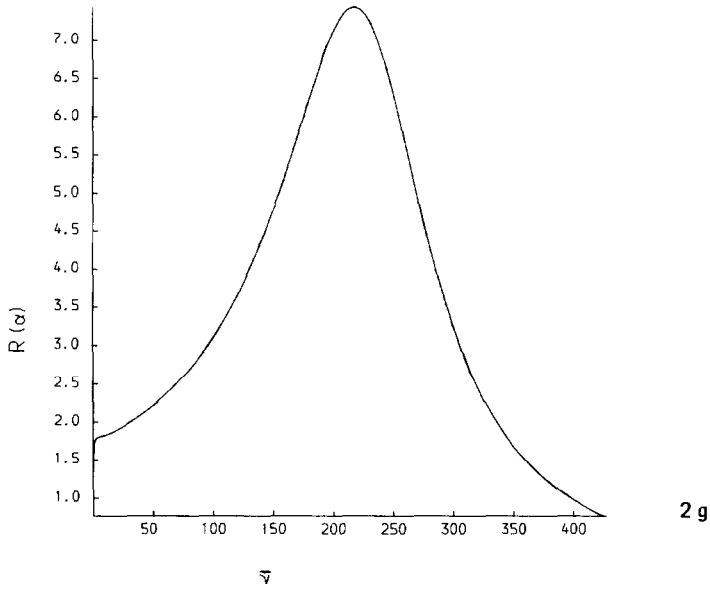


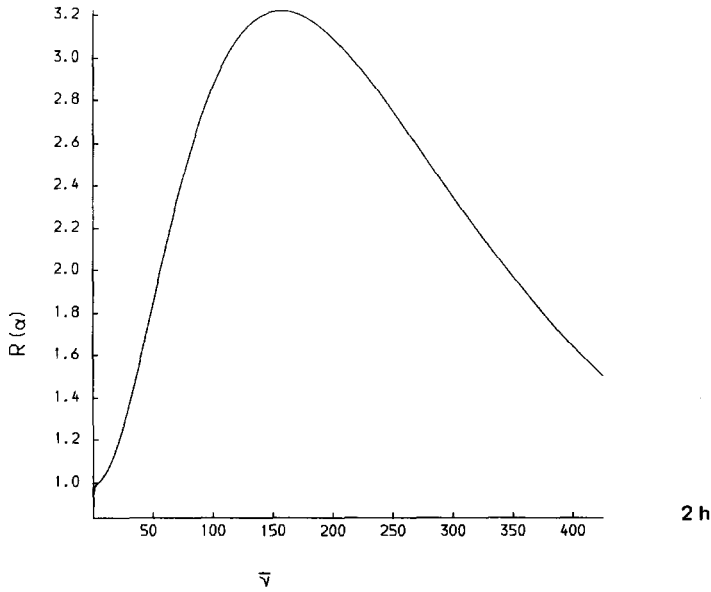
Fig. 2.

$$\alpha=8, \beta=10, \gamma=10, N=2$$



2 g

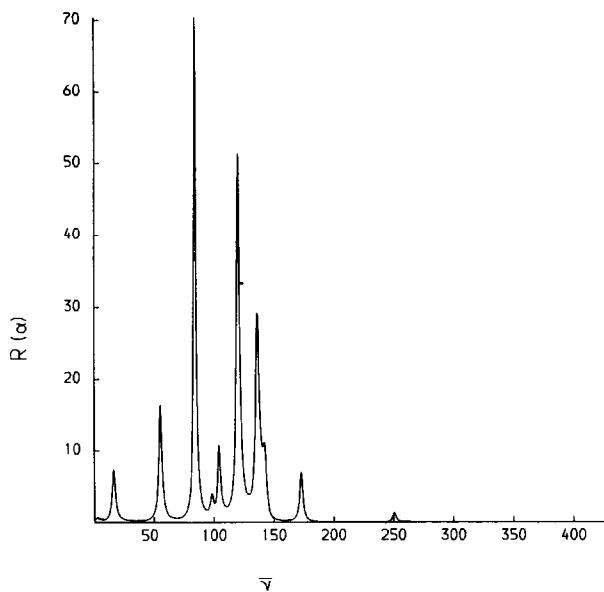
$$\alpha=8, \beta=50, \gamma=10, N=2$$



2 h

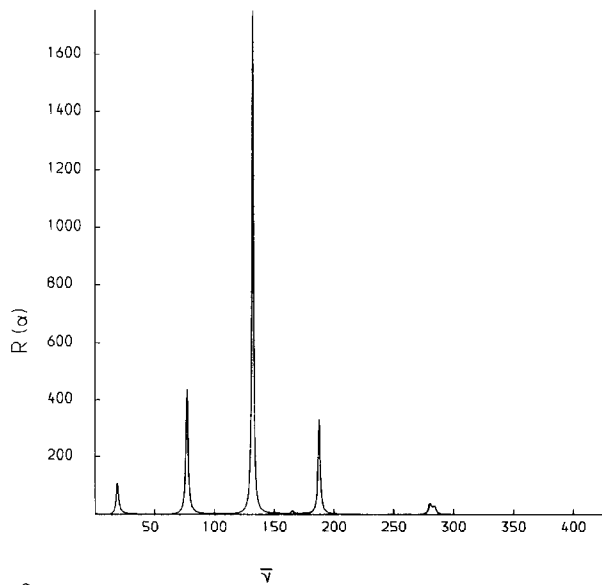
Fig. 2.

$\alpha=5, \beta=0.07, \gamma=5, N=2$



3 a

$\alpha=10, \beta=0.05, \gamma=5, N=2$



3 b

Fig. 3.

$$\alpha=10, \beta=0.05, \gamma=10, N=2$$

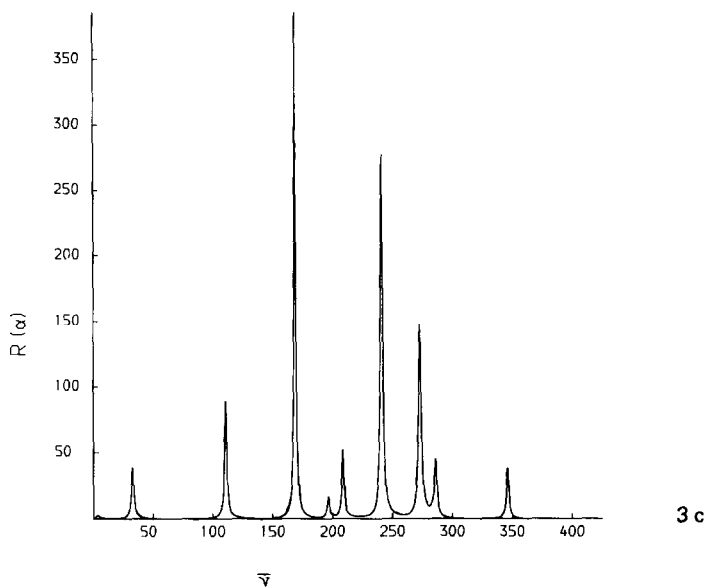


Fig. 3 The effect of varying $\alpha = (kT/I)^{\frac{1}{2}}$

lengthens. In the low friction limit, however (fig. (4)), the behaviour is far more complicated, especially in the far infra-red, and we refer the reader to the computer graphics of fig. (4) for a detailed description.

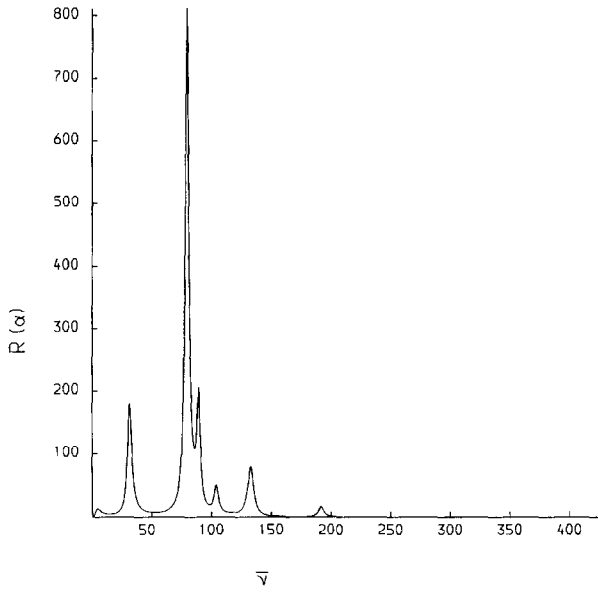
To end this section we note that none of the panels in figs. (2) to (4) exactly reproduce the experimental data of fig. (1), are not intended for this purpose and cannot be expected to do so because of the extreme limit in simplicity chosen for the effective (cosine) potential wells and because $M = 2$ only. However, improvements between theoretical description and observed spectra could be obtained by increasing the well multiplicity from $M = 2$ and by incorporating a detailed and realistic description of the local structure that is known to exist in this liquid. Unfortunately the expansion used by Reid for the p.d.f.:

$$\rho(\dot{\theta}, \theta, t) = \exp\left(\frac{-\dot{\theta}^2}{4\alpha^2}\right) \sum_{n=0}^{\infty} D_n\left(\frac{\dot{\theta}}{\alpha}\right) \phi_n(\theta, t) \quad (11)$$

causes convergence problems for $M > 2$ in the limit $\beta \rightarrow 0$, and also for

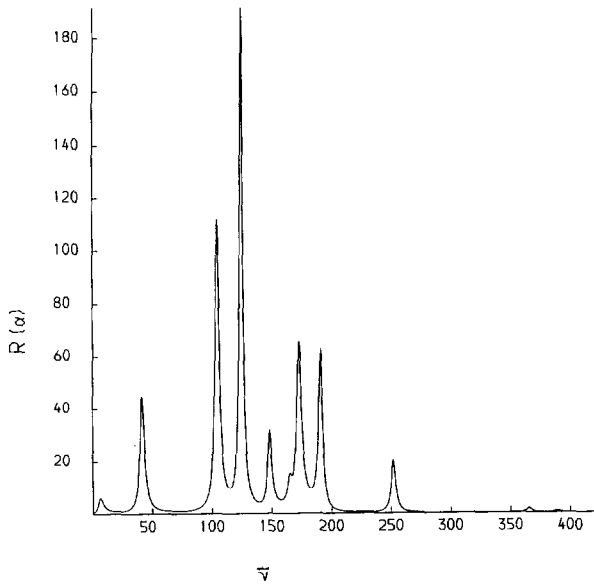
12

$\alpha=8, \beta=0.1, \gamma=2, N=2$



4 a

$\alpha=8, \beta=0.1, \gamma=6, N=2$



4 b

Fig. 4.

$$\alpha=8, \beta=0.1, \gamma=8, N=2$$

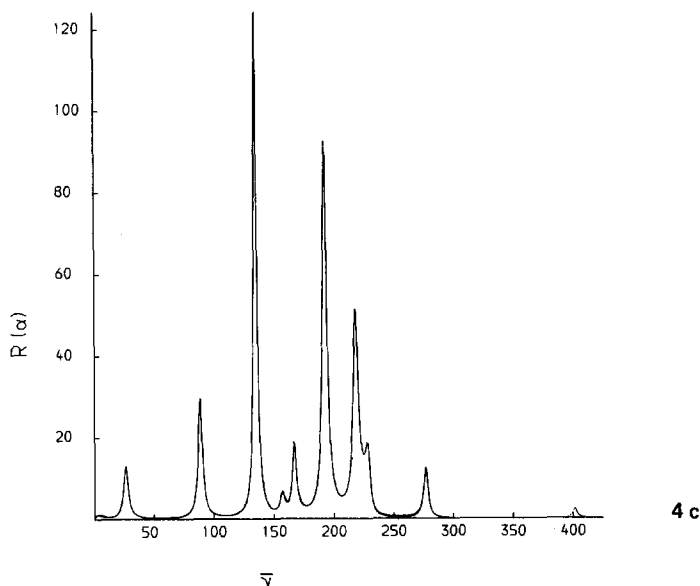


Fig. 4 Variation of $\gamma = V_0 / (IkT)^{\frac{1}{2}}$

$\gamma \gg \alpha$. In eqn. (11) D_n are the Hermite polynomials [2,4,7] and ϕ_n is itself expanded into a Fourier series:

$$\phi_n(\theta, t) = \sum_{p=-\infty}^{\infty} A_p^n(t) \exp(ip\theta)$$

It is desirable to increase the multiplicity M from $M = 2$ to $M = 7 \pm 1$ (in accord with structural information on CH_3CN) in the limit $\beta \rightarrow 0$ because it is expected that this would lead under certain conditions to a dense panoply of theoretical fine structure (hundreds of far infra-red peaks) producing an overall effect similar to what is actually observed (fig. (1)), i.e. fine structure above what appears to be a broad background. (In a sense all far infra-red spectra of dipolar liquids [1] must be dense panopies of this type).

There is an algorithm available for this purpose, based on the adiabatic elimination and continued fraction procedures of the Pisa group of Grigolini, Pastori and co-workers [7] which does not depend on the diagonalisation of large

matrices and can be used for solving classes of Kramers and master equations in a variety of disciplines. The application of this algorithm to the problem of far infra-red fine structure, or shoulders in what was previously thought to be a broad band, will be the subject of future work. In the remaining section of this paper we concentrate on the effect of an external electric field [15], i.e. the spectra produced by the solution of eqn. (10). This introduces a further variable (ω_1) into the analysis and produces a variety of unexpected effects, corroborating qualitatively the indications obtained experimentally by G.J. Evans [12] in the far infra-red (fig. (1)).

The Effects of an External Electric Field

This is illustrated in fig. (5) through the dielectric loss and power absorption coefficients, as a function of ω_1 for $\alpha = 8$ THz, $\gamma = 10$ THz, $\beta = 0.1$ THz and $M = 2$. These results are numerical solutions of eqn. (10) for the real part of $\epsilon''(\omega)$ and the real part of $\alpha(\omega)$.

$\alpha=8, R(\beta)=0.1, \text{Im}(\beta)=-0.2, -0.5, -1, \gamma=10, N=2$

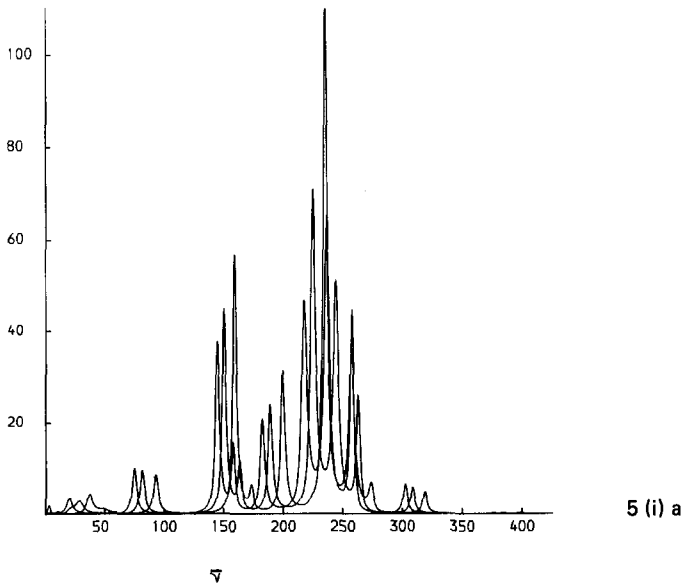
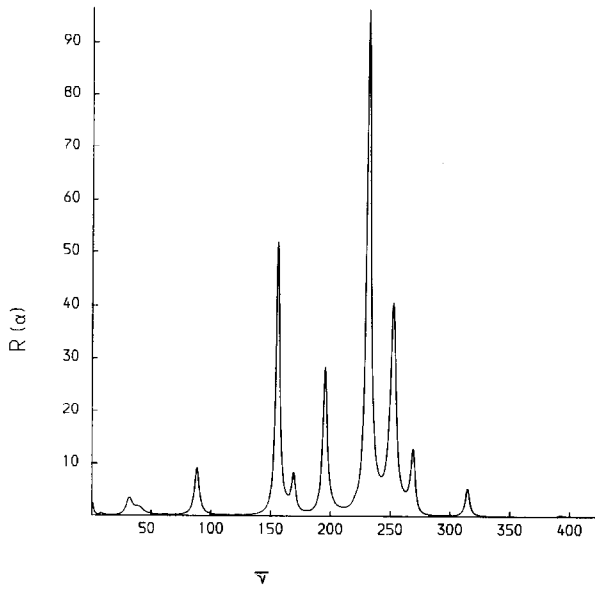


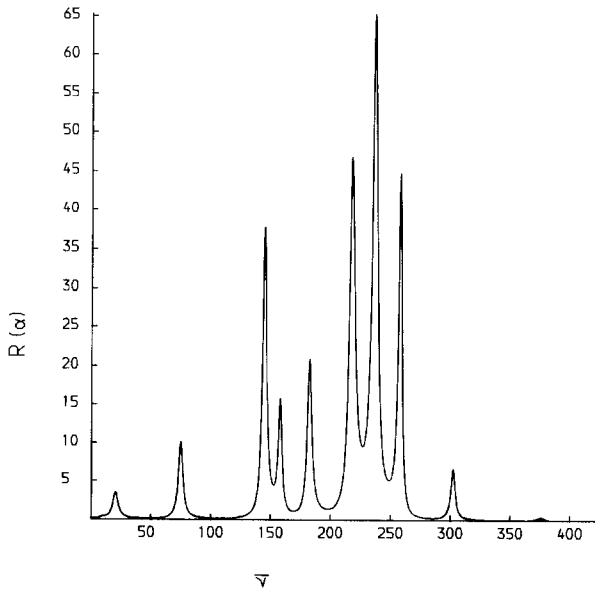
Fig. 5. The effect of increasing $\omega_1 = (\mu E/I)^{1/2}$ on (i) the power absorption coefficient from eqn. (10); (ii) the dielectric loss. The value of ω_1 is indicated in the complex negative entry for β on the computer graphics.

$$\alpha=8, \beta=(0.1, -0.08), \gamma=10, N=2$$



5 (i) b

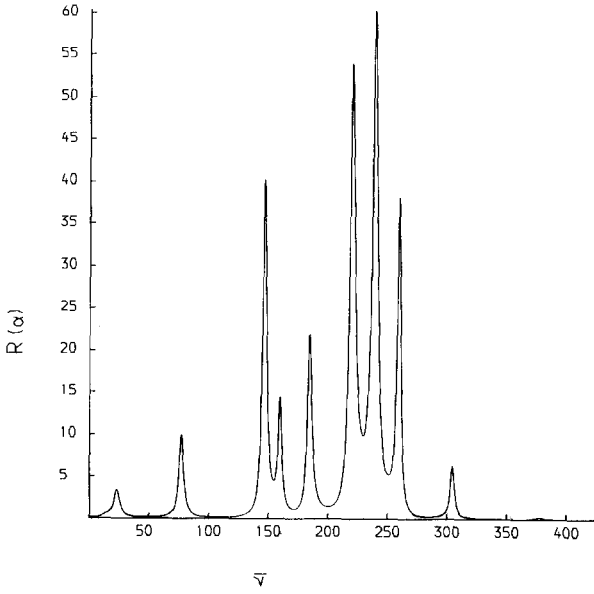
$$\alpha=8, \beta=(0.1, -0.2), \gamma=10, N=2$$



5 (i) c

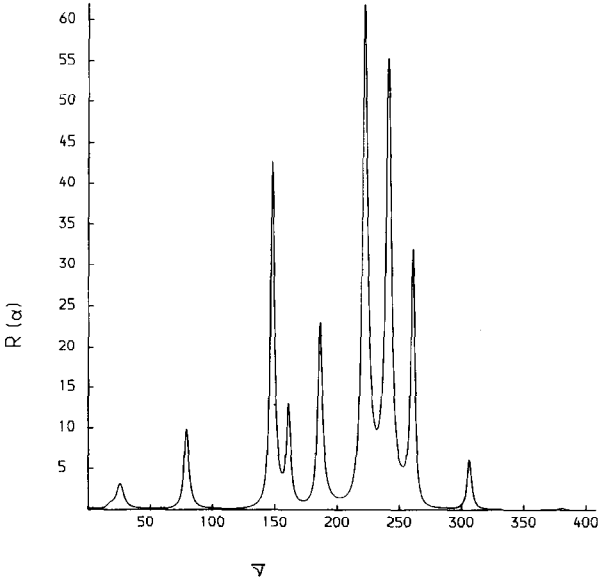
Fig. 5.

$\alpha=8, \beta=(0.1, -0.3), \gamma=10, N=2$



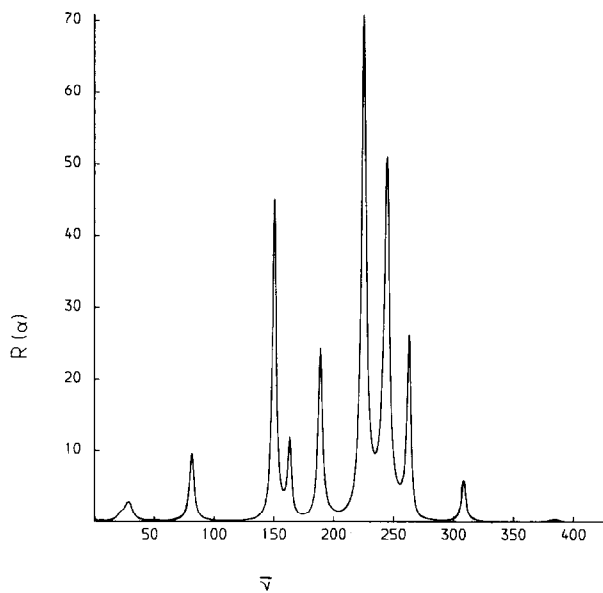
5 (i) d

$\alpha=8, \beta=(0.1, -0.4), \gamma=10, N=2$

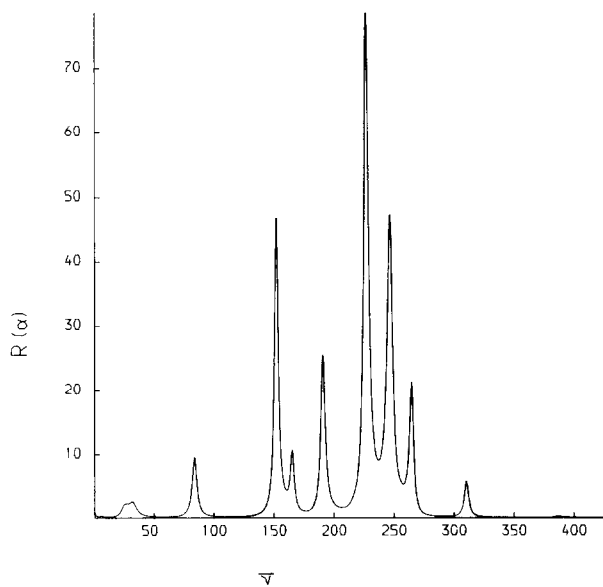


5 (i) e

Fig. 5.

$\alpha=8, \beta=(0.1, -0.5), \gamma=10, N=2$ 

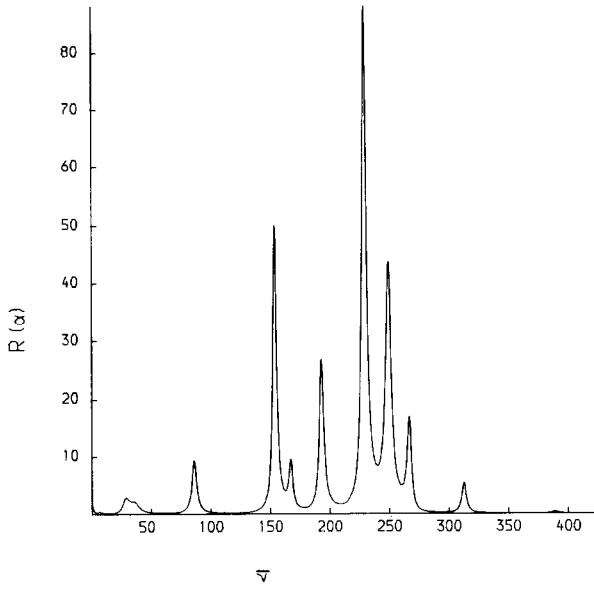
5 (i) f

 $\alpha=8, \beta=(0.1, -0.6), \gamma=10, N=2$ 

5 (i) g

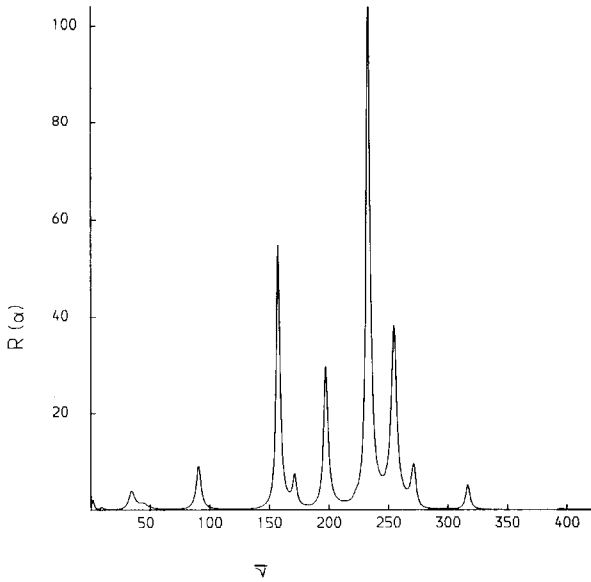
Fig. 5.

$\alpha=8, \beta=(0.1, -0.7), \gamma=10, N=2$



5 (i) h

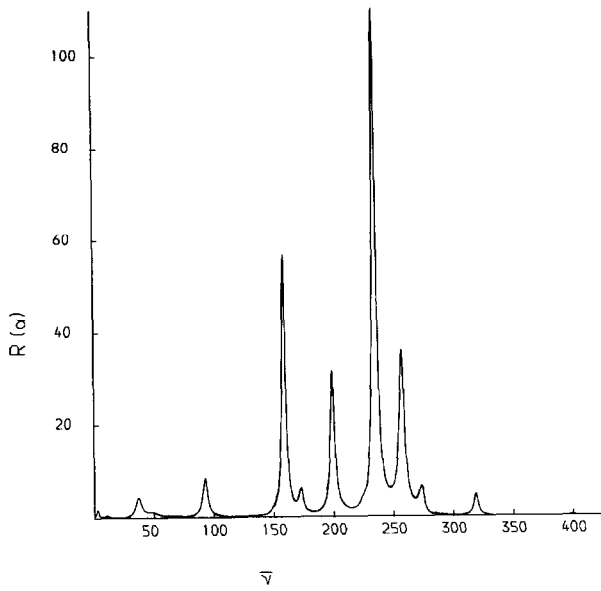
$\alpha=8, \beta=(0.1, -0.9), \gamma=10, N=2$



5 (i) i

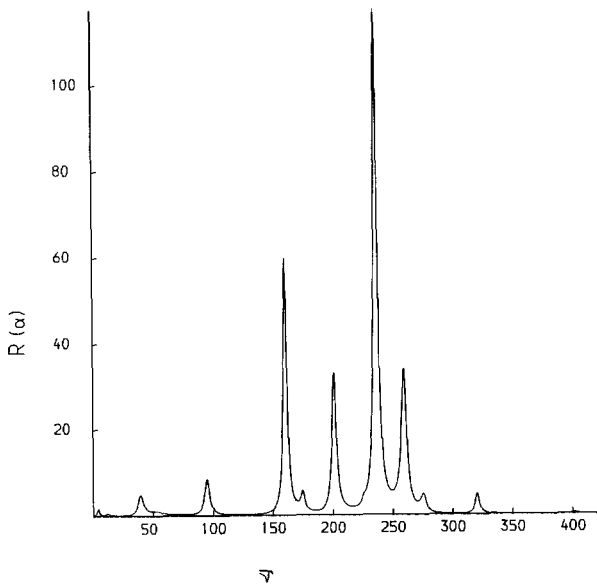
Fig. 5.

$$\alpha=8, \beta=(0.1, -1.0), \gamma=10, N=2$$



5 (i) j

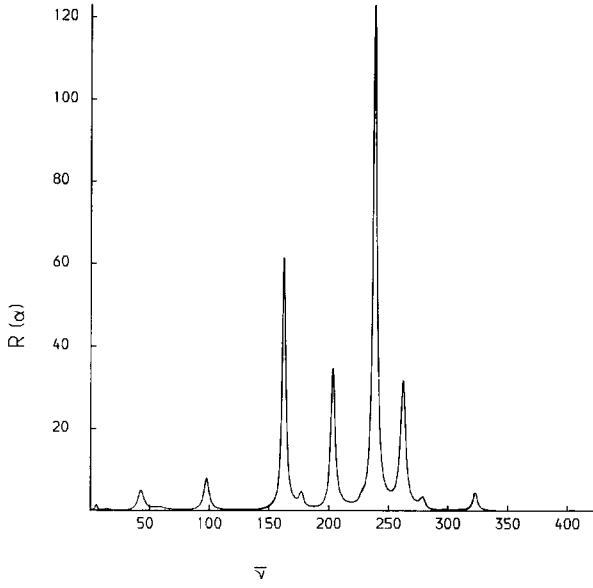
$$\alpha=8, \beta=(0.1, -1.1), \gamma=10, N=2$$



5 (i) k

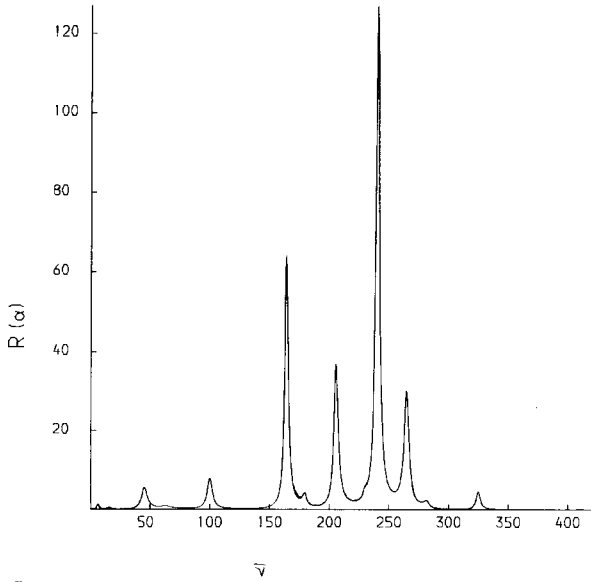
Fig. 5.

$\alpha=8, \beta=(0.1, -1.2), \gamma=10, N=2$



5 (i) l

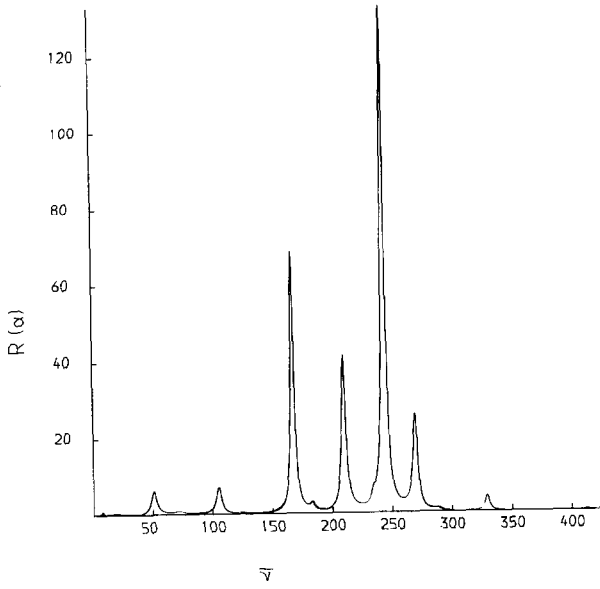
$\alpha=8, \beta=(0.1, -1.3), \gamma=10, N=2$



5 (i) m

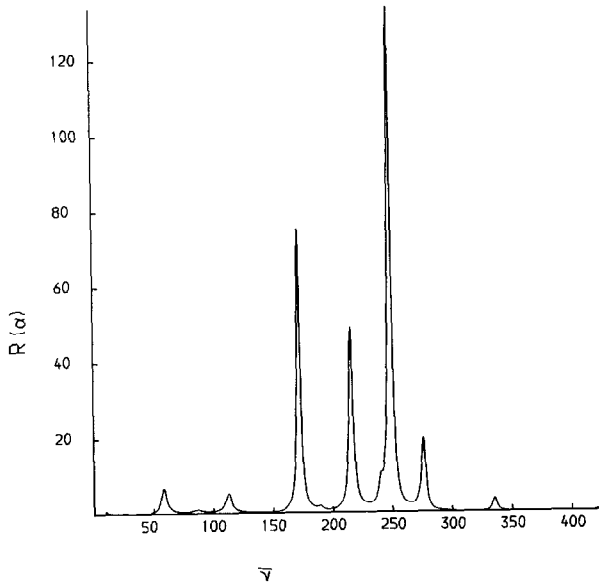
Fig. 5.

$\alpha=8, \beta=(0.1, -1.5), \gamma=10, N=2$



5 (i) n

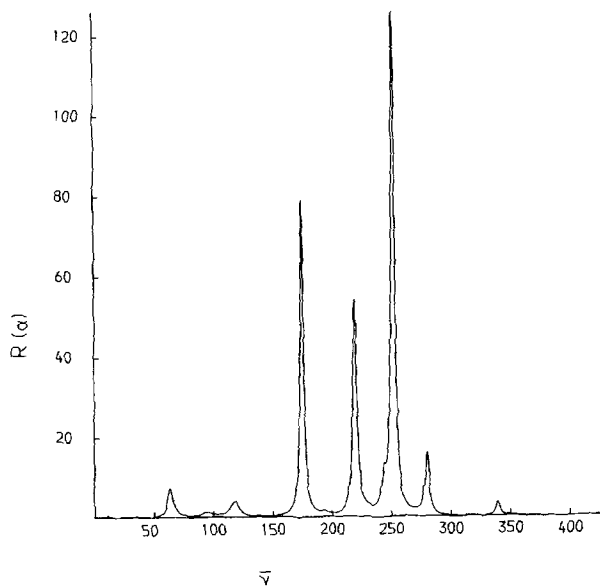
$\alpha=8, \beta=(0.1, -1.8), \gamma=10, N=2$



5 (i) o

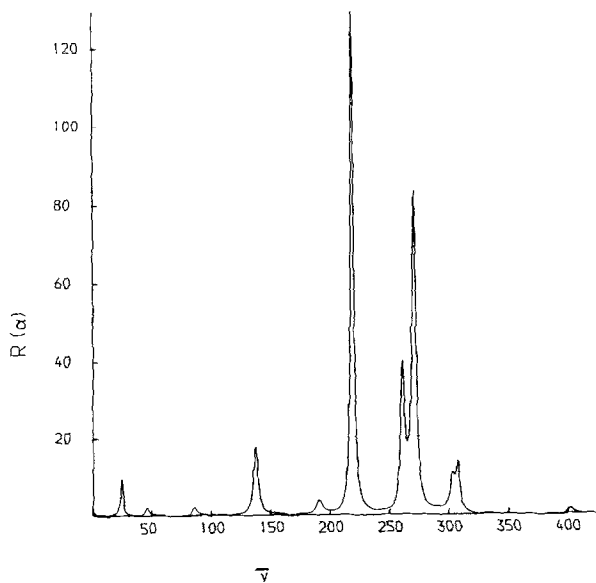
Fig. 5.

$$\alpha=8, \beta=(0.1, -2.0), \gamma=10, N=2$$



5 (i) p

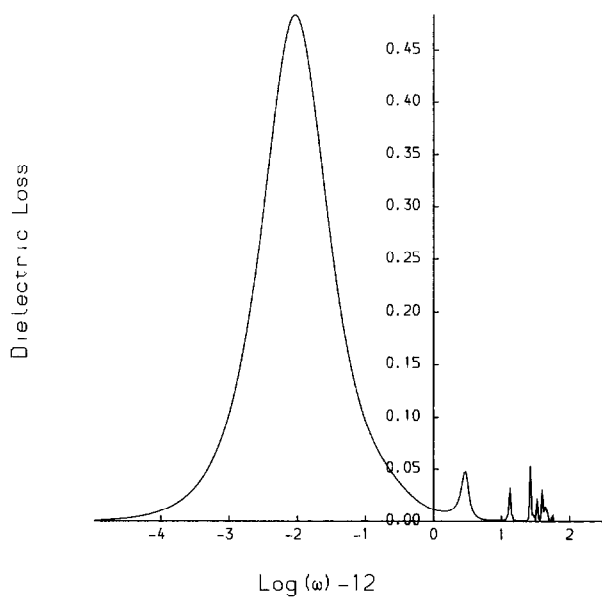
$$\alpha=8, \beta=(0.1, -5), \gamma=10, N=2$$



5 (i) q

Fig. 5.

$$\alpha=8, \beta=(0.1, -0), \gamma=10, N=2$$



$$\alpha=8, \beta=(0.1, -0.8), \gamma=10, N=2$$

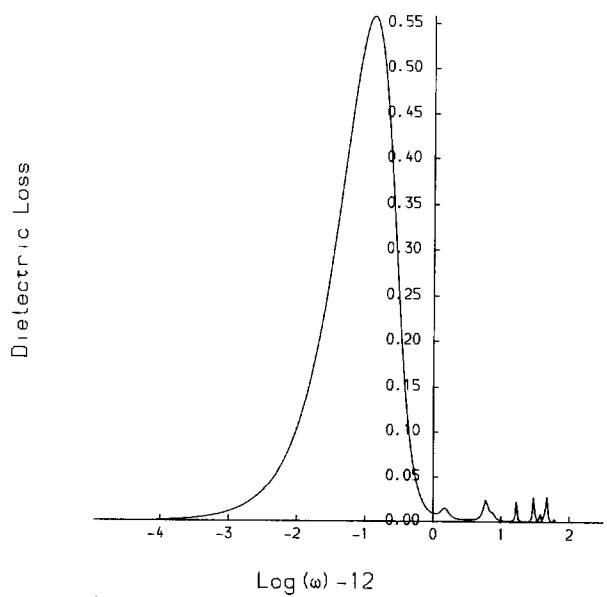
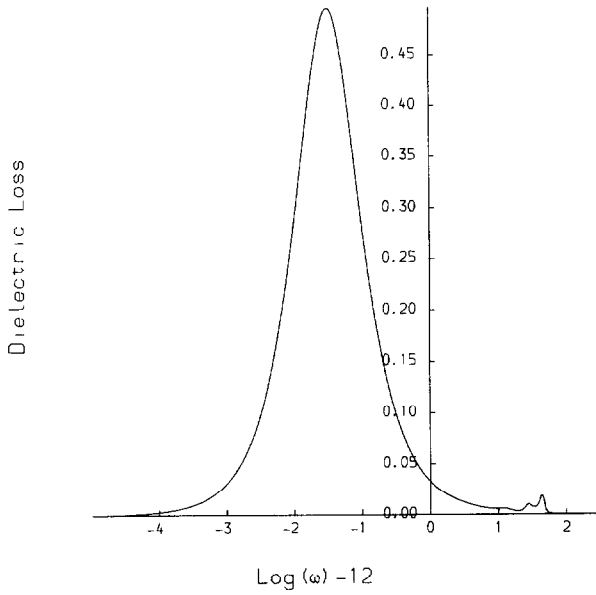


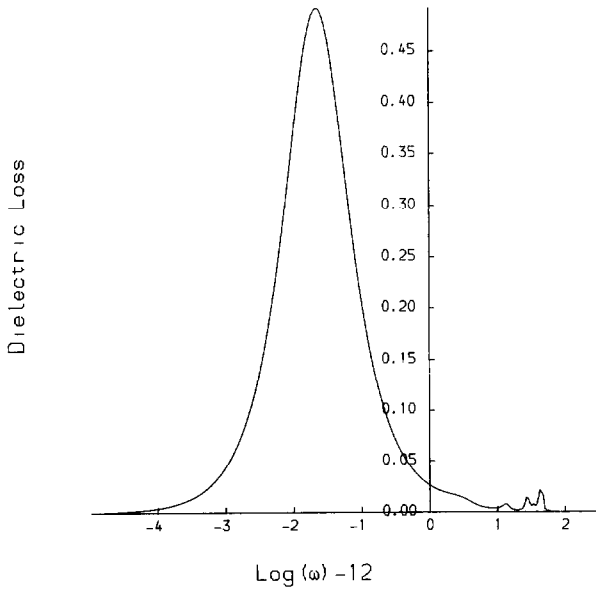
Fig. 5.

$$\alpha=8, \beta=(1.0, 0), \gamma=10, N=2$$



5 (ii) c

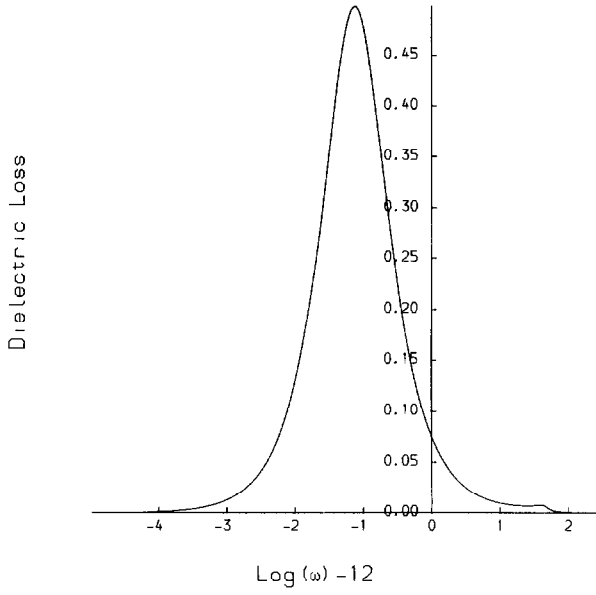
$$\alpha=8, \beta=(0.5, 0), \gamma=10, N=2$$



5 (ii) d

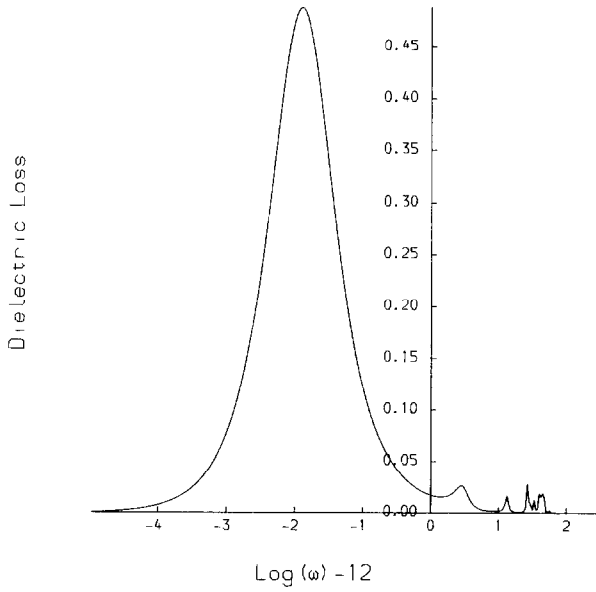
Fig. 5.

$\alpha=8, \beta=(10, 0), \gamma=10, N=2$



5 (ii) e

$\alpha=8, \beta=(0.2, 0), \gamma=10, N=2$



5 (ii) f

Fig. 5.

The effect of increasing ω_1 on the dielectric loss is unprecedented by anything recorded [1,19] in the high friction (Debye) limit. As ω_1 is increased from zero to about 0.5 THz the dielectric loss ϵ'' as a function of $\log_{10}(\omega)$ sharpens and shifts to higher frequencies. For 0.5 THz $\lesssim \omega_1 \lesssim$ 1.0 THz, however, the dielectric loss broadens once more, and is clearly asymmetric at about $\omega_1 = 0.8$ THz (fig. 6). Thereafter it broadens considerably and splits into two distinct broad bands (recall the log scale on the abscissa) at $\omega_1 = 1.0$ THz. The splitting process is best described as the appearance and development of another very broad loss process at lower frequencies from the asymmetric low frequency tail of the loss at $\omega_1 = 0.8$ THz. A separate panel of fig. (6) illustrates the development of a "second cycle" as ω_1 is increased from 1.0 THz to about 4.0 THz. The cycle is similar to the first process mentioned already ($0 < \omega_1 < 1.0$ THz). In the region 1.0 THz $\lesssim \omega_1 \lesssim$ 4.0 THz however the loss peaks are sharper and the second cycle peaks at a higher frequency ω . At about $\omega_1 = 4.0$ THz a secondary lower frequency loss process appears again which is broader than in the first cycle, and peaks at

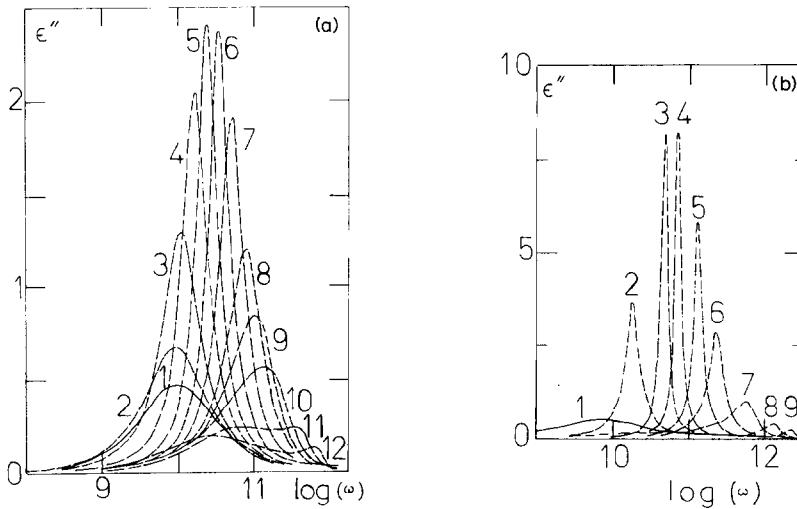


Fig. (6) The loss cycles. (a) cycle 1. 1) $\omega_1 = 0$ THz; 2) 0.1 THz; 3) 0.2 THz; 4) 0.3 THz; 5) 0.4 THz; 6) 0.5 THz; 7) 0.6 THz; 8) 0.7 THz; 9) 0.75 THz; 10) 0.8 THz; 11) 0.9 THz; 12) 1.0 THz.
 (b) Cycle 2. 1) $\omega_1 = 1.2$ THz (nearly Debye); 2) 1.5 THz; 3) 2.1 THz; 4) 2.6 THz; 5) 3.0 THz; 6) 3.25 THz; 7) 3.5 THz; 8) 3.75 THz; 9) 4.0 THz.

slightly lower ω . The whole process then goes into a third and more cycles for $\omega_1 \gtrsim 4.0$ THz. The equivalent effect on the far infra-red power absorption coefficients is best described graphically (fig. (5)), and clearly, ω_1 has a profound influence on the far infra-red fine structure from eqn. (10). In the high field limit [15] ($\omega_1 \rightarrow \infty$) the far infra-red power absorption from eqn. (10) becomes concentrated in one or two intense peaks.

The equivalent experimental results in fig. (1) show that the effect of an electric field strength in the kv cm^{-1} region* on liquid acetonitrile is to sharpen the peak structure and to narrow the overall profile. The results from eqn. (10) again do not reproduce the experimental data in the specific case of acetonitrile precisely, as expected, but are a qualitative corroboration of the experimental observation. (In this context it is worth mentioning that considerable fine structure in the far infra-red spectrum of a liquid crystal has been reported by Evans and Evans [20], together with pronounced electric field effects in liquid aniline [21]. Gerschel [22] has reported some broader structure in highly dipolar media such as liquid CH_3Cl [23]. The experimental results by G.J. Evans [12] in the absence of external fields are being re-measured by Birch et al. [24] at the U.K. National Physical Laboratory. However there is a pressing need now for high resolution, high precision experimentation using state of the art spectrometers to pursue these observations further).

Suggestions for Further Work

The appearance of fine detail in liquid state infra-red power absorption cannot be accounted for without proper consideration of the effect of liquid structure on molecular dynamics using the Kramers diffusion equation. A solution of this equation with a realistic multiplicity of about 7 should produce a large number of sharp far infra-red peaks, as observed experimentally. Future theoretical work will concentrate on improving the convergence of the algorithms available [7] to solve the Kramers equation and achieve the aim.

* $\omega_1 = 1.0$ THz for $I = 10^{-40}$ g cm^2 corresponds to an electric field strength of 100 volts cm^{-1} for $\mu = 1.0$ D.

In experimental terms the results available to date [1,2] on far infra-red broad band spectroscopy should be re-examined at high resolution for signs of shoulders or fine detail. It would be particularly interesting to make a detailed study of liquids with a low viscosity and high residual structure; namely acetonitrile and analogues, and nematic liquid crystals [20,12].

ACKNOWLEDGEMENTS

The University of Wales is thanked for a Fellowship (to M.W.E.). Dr. F. Marchesoni and Professor P. Grigolini are acknowledged for suggesting the use of the cosine model to generate f.i.-r. sub-structure. SERC is thanked for the award of an Advanced Fellowship to G.J.E. The original motivation for this work came from Dr. W.T. Coffey, Trinity College, Dublin.

REFERENCES

- 1 E.g. M.W. Evans, G.J. Evans, W.T. Coffey and P. Grigolini, "Molecular Dynamics", Wiley/Interscience, N.Y., 1982, Chapters 1,4,6,11.
- 2 W.T. Coffey, M.W. Evans and P. Grigolini, "Molecular Diffusion", Wiley/Interscience, N.Y., 1984, Chapters 3 - 6.
- 3 H. Nelson, "Dynamical Theories of Brownian Motion", Princeton Univ. Press, Princeton, N.J., 1967.
- 4 For a review, see ref. (1), Chapter 2.
- 5 G.E. Uhlenbeck and L.S. Ornstein, Phys. Rev., 36, (1930) 823.
- 6 H.A. Kramers, Physica, 7, (1940) 284.
- 7 "Memory Function Approaches to Stochastic Problems in Condensed Matter", a two volume special issue of Adv. Chem. Phys., ed. M.W. Evans, P. Grigolini and G. Pastori-Parravicini, Series ed. Prigogine and Rice, in press, Vol. 1.
- 8 C.J. Reid, Mol. Phys., 49, (1983) 331.
- 9 E. Praestgaard and N.G. van Kampen, Mol. Phys., 43, (1981) 33.
- 10 H. Risken and H.D. Vollmer, Z. Phys., B, 31, (1978) 209.
- 11 M.W. Evans, M. Ferrario and W.T. Coffey, Adv. Mol. Rel. Int. Proc., 20, (1981) 1.
- 12 G.J. Evans, J. Chem. Soc., Faraday Trans. II, 79, (1983) 547.
- 13 O. Steinhauser and H. Bertagnolli, Chem. Phys. Lett., 78, (1981) 555
- 14 For a review see M.W. Evans, J. Mol. Liq., 25, (1983) 149
G.J. Evans and M.W. Evans, Adv. Chem. Phys., in press (1984);
G.J. Evans, Adv. Chem. Phys., in press, 1984.

- 15 See ref. (2), Chapter 9.
- 16 J.K. Eloranta and P.K. Kadaba, *Trans. Faraday Soc.*, 66, (1970) 817
- 17 E. Krishnaji and A. Mansingh, *J. Chem. Phys.*, 41, (1964) 827
- 18 C.A. Chatzidimitriou-Dreismann and E. Lippert, *Ber. Buns. Ges. Phys. Chem.*, 84, (1980) 775.
- 19 M. Davies, A.H. Price, N.E. Hill and W.E. Vaughan, "Dielectric Properties and Molecular Behaviour", van Nostrand, N.Y. (1969).
- 20 G.J. Evans and M.W. Evans, *J. Chem. Soc., Chem. Comm.*, (1978) 267.
- 21 M.W. Evans and G.J. Evans, *J. Chem. Soc., Faraday Trans. II*, 76 (1980).
- 22 A. Gerschel, personal communication.
- 23 For a review, see M.W. Evans, *J. Mol. Liq.*, 25, (1983) 211
- 24 J. Birch, personal communication.